Title
OPTIMUM LUMPED PARAMETERS FOR MODELING THE THERMAL PERFORMANCE OF BUILDINGS

Author
Richardson, R.W.

Publication Date
1980-09-01

EEB-W-79-20
W-46

LBL-9588 Preprint

Lawrence Berkeley Laboratory
UNIVERSITY OF CALIFORNIA

ENERGY & ENVIRONMENT DIVISION

Submitted to the International Journal of Ambient Energy

OPTIMUM LUMPED PARAMETERS FOR MODELING THE THERMAL PERFORMANCE OF BUILDINGS

R.W. Richardson and S.M. Berman

September 1980

Prepared for the U.S. Department of Energy under Contract W-7405-ENG-48

DISCLAIMER

W-46
LBL-9588
EEB-W-79-20

OPTIMUM LUMPED PARAMETERS FOR MODELING THE THERMAL PERFORMANCE OF BUILDINGS

R. W. Richardson* and S. M. Berman

Energy and Environment Division
Lawrence Berkeley Laboratory
University of California
Berkeley, CA 94720

September 1980

The work described in this report was funded by the Office of Buildings and Community Systems, Assistant Secretary for Conservation and Solar Applications of the U.S. Department of Energy under contract No. W-7405-ENG-48.

*Permanent address: Physics Department, New York University, 4 Washington Place, New York, NY 10003.

LBL-9588

OPTIMUM LUMPED PARAMETERS FOR MODELING THE THERMAL PERFORMANCE OF BUILDINGS

R. W. Richardson* and S. M. Berman

Energy and Environment Division
Lawrence Berkeley Laboratory
University of California
Berkeley, California 94270

ABSTRACT

A least-squares method for choosing optimum lumped parameters for modeling the thermal performance of buildings is presented. A realistic passive solar heated room is modeled with a one-time constant lumped model to better than 10% accuracy. This technique provides a simple method that can be used in the design or evaluation of the thermal performance of buildings such as those using passive solar heating.

*Permanent address: Physics Department, New York University, 4 Washington Place, New York, NY 10003.

I. INTRODUCTION

In order to conserve energy, buildings must be built so as to make the best use of their various sources of thermal energy. This objective can only be achieved if designers or standards writers can relate the physical properties of the building to its thermal performance in a transparent fashion. In this paper, we present a simple method for carrying out this relationship and show, by applications to a room with passive solar heating and one with a heater, that the method is sufficiently accurate. This method will be useful both as a design tool and as a means for evaluating the impact of building standards.

Many approximations must be made in order to formulate a tractable set of equations describing the temperature of a complex structure such as a building. The assumptions of one-dimensional heat flow, perfectly mixed interior air, and idealized thermal elements are common among these approximations. While a detailed assessment of the validity of these approximations has not been made, they cannot be expected to be more than ten percent accurate. Once the equations have been formulated, one is faced with the task of solving them. Here, one can choose numerical or analytical, approximate or exact methods. In this paper, we present an approximate analytical method for solving the equations whose accuracy is comparable to the accuracy with which the original equations model the real world structure.

Before describing our method, we classify the types of heat sources or stimuli that drive the temperature of a building. We place them in two categories. In the first category are those sources that can be well represented by a few Fourier components such as the diurnal variations of the ambient temperature. These sources can be efficiently dealt with by Fourier series methods and will not concern us here. The sources in the second category change abruptly with time and require many Fourier components for their representation. Examples of such sources would be the sunshine falling on the collector of a passive solar house or a pulse of heat from an internal heater. We will only consider sources of the second category in what follows. Since the temperature is linearly related to the heat sources, it can be represented as a sum of terms, each term arising from a particular source, when there is more than one heat source present.

Our technique is a method for choosing the parameters in a lumped parameter approximation to the original continuum equations. Any such approximation should have the following attributes:

1. It must be simple, for this is its only reason for being.
2. It must involve both the structure being simulated and the stimulus that is applied to it. One can easily visualize pathalogical situations in which a given structure is best simulated by very different parameters due to differences in the stimulus. For example, compare the results of Secs. II and III.
3. The method must be accurate and it should yield an error estimate.
4. It should be possible to systematically improve the approximation if the error estimate is unacceptably large.

The method we present shares all of these attributes.

We choose the parameters in our lumped parameter approximation to a set of "exact" continuum equations so that the approximate temperature is a least-squares fit to the exact temperature. This fit is done in frequency--rather than time--space since both exact and approximate equations can be easily solved for a given frequency. The most important output, however, is the approximate temperature as a function of time. In performing this fit, we find that it is very important to separate the static and dynamic responses of the temperature. In the examples we treat, the average temperature is fitted exactly and the fluctuations about the average are fitted in the least-squares sense. This separation yields values for the dynamic lumped parameters that are very different from the static ones.

We treat an example in detail as an introduction and test of the method. It is meant to model a room with passive solar heating. The least-squares fit to the temperature yields a natural root-mean-square error as an error estimate, and we find that it is about 10% of the mean or less for the examples treated. Since these examples were chosen so as to be a severe test of the method (the root-mean-square variation of the temperature about the mean is 63-98% of the mean) we believe that this is a generous estimate of the errors. We also present a very simple approximation to the root-mean-square fit which yields results that are very close to the best fit.

The method and passive-solar example are treated in parallel in Sec. II. A second example of a room with a heat source that delivers a pulse of heat is treated in Sec. III. Comments and conclusions are given in Sec. IV.

Our method is not intended to compete with the large computer programs[1] used in building simulations. Properly used, it would compliment the detailed results that they produce. Our method gives a simple qualitative relationship between building design parameters and thermal performance rather than a detailed response of a particular design to a specific pattern of use. Given the uncertainties in the basic equations, construction practices, and use and weather patterns, this may be sufficient information for the designer. Background information on heat transfer and environmental engineering may be found in Ref. 2. A rudimentary lumped parameter model is considered in Ref. 3.

II. DETERMINATION OF PARAMETERS

In general, the sources of heat in a building can be placed in one of two categories. They are either smoothly varying in time and can be well represented by a few terms in a Fourier series or they are rapidly varying and require many terms for an accurate representation. The response of the building to the smoothly varying sources of the first kind can be calculated using standard Fourier techniques. Here, we are concerned with modeling the response to the rapidly varying sources. This is done by constructing a lumped parameter model of the building and choosing optimum values for the parameters. The choice is done so as to minimize the mean square errors of the model temperature. In this section, we develop this method of parameter choice while treating a specific model in detail as an example. We also consider a simple approximate choice of parameters which yields results that are almost as good as the optimum. We find that a simple model with a single time constant can predict the performance of a complex structure with errors of the order of 10%. However, the values of the optimum parameters are very different form those obtained by "physical" arguments based upon the static response of the structure.

We consider the temperature of a room T_R that is surrounded by thermal elements and subjected to a periodic heat source. In order to be specific, we assume that the fundamental period is one day, P = 24 hours, although this is not at all necessary and variations in the weather can be easily taken into account. In general, the heat source can be characterized by some source temperature T_S, e.g., as the heat rate divided by some charcteristic heat conductance of the room.

Then, by the assumed periodicity of the source, we can write

$$T_S(t) = \sum_{n=-\infty}^{\infty} T_{Sn}\, e^{in\omega t} \quad , \tag{2.1}$$

where $\omega = 2\pi/P$ and T_{Sn} the Fourier coefficients of the source T_S. Since T_S is real, we must have $T_{Sn} = T^{*}_{S-n}$. The room temperature response to the source (2.1) T_R will also be periodic with Fourier coefficients T_{Rn}. No matter how complex the structure is, this response will be linear and we can write

$$T_{Rn} = \chi_n T_{Sn} \quad , \tag{2.2}$$

where χ_n depends upon the structure. Since T_R is real, we have $\chi_n = \chi^{*}_{-n}$ and since causes must precede effects, we have the imaginary part of χ_n is negative for positive n. We therefore write χ_n as

$$\chi_n = \chi'_n - i\,\chi''_n \quad , \tag{2.3}$$

where the real part of χ_n, χ'_n, is an even function of n and the negative imaginary part χ''_n is an odd function of n which is positive for positive n.

In order to make the above considerations more concrete, we consider a specific example which we will carry along throughout this section. The example is a simplified model of a room with passive solar heating. It consists of an outer wall and an inner wall. Sunshine is incident upon the inner wall, and one dimensional heat flow takes place between the walls, room, and outer environment. This is pictured in Fig. 2.1. This can be taken as a very simplified model of a room which has no heat conduction through the three interior walls and floor, which are modeled by the "inner" wall, but looses heat through the outer wall and roof which are modeled by the "outer" wall. The assumption of one-dimensional heat flow neglects temperature variations at the corners of the walls and throughout the air in the room. One can easily sophisticate the model by adding thermal elements and/or modifying the boundary conditions. However, it is very hard to get around the assumption of one-dimensional heat flow without an undue amount of additional computation.

Quantities pertaining to the outer wall are denoted by a subscript "1". It has a U-value U_1, a heat capacity per unit area C_1, and thickness d_1. The temperature distribution in this wall is $T_1(\xi_1,t)$, where $\xi_1 = X_1/d_1$ and X_1 the position in the wall measured from the outer surface. The one dimensional heat flow in this wall is governed by the diffusion equation

$$\frac{\partial T_1}{\partial t} = \Lambda_1 \frac{\partial^2 T_1}{\partial \xi_1^2}, \qquad (2.4)$$

where $\Lambda_1 = U_1/C_1$ is the decay constant for the wall.
We measure all the temperatures with respect to the outside temperature and assume that the outer wall is strongly coupled to the outside air so that the outer boundary condition is

$$T_1(\xi_1 = 0, t) = 0. \qquad (2.5)$$

We assume that the inner surface of the outer wall is coupled to the room temperature T_R through a film coefficient h so that the inner boundary condition is

$$- \frac{\partial T_1(\xi_1 = 1, t)}{\partial \xi_1} = \eta_1 \left[T_1(\xi_1 = 1, t) - T_R(t) \right] , \tag{2.6}$$

where $\eta_1 = h/U_1$.

These equations determine the temperature of the outer wall T_1.

Quantities pertaining to the inner wall are denoted by a subscript "2". It has a U-value U_2, a heat capacity per unit area C_2 and a thickness d_2. The temperature distribution in this wall is $T_2(\xi_2, t)$, where $\xi_2 = X_2/d_2$ and X_2 is the position in the wall. It satisfies the diffusion equation

$$\frac{\partial T_2}{\partial t} = \Lambda_2 \frac{\partial^2 T_2}{\partial \xi_2^2} , \tag{2.7}$$

where $\Lambda_2 = U_2/C_2$ is the decay constant for this wall. We assume that the inner surface of this wall is coupled to the room temperature through a film coefficient h (taken to be the same for both walls for simplicity) and that there is a solar flux S(t) incident upon it. The inner boundary condition is

$$- \frac{\partial T_2(\xi_2 = 0, t)}{\partial \xi_2} = \eta_2 \left[T_R(t) - T_2(\xi_2 = 0, t) + T_S(t) \right] \tag{2.8}$$

where $\eta_2 = h/U_2$ and $T_S(t) = S(t)/h$ is the characteristic temperature of the solar heat flux. The outer surface of this wall is assumed to be perfectly insulated so that the boundary condition is

$$\frac{T_2(\xi_2 = 1, t)}{\partial \xi_2} = 0 . \tag{2.9}$$

These equations determine the temperature distribution in the second wall.

The room is assumed to have a heat capacity per unit area C_R and temperature T_R which, as stated above, is coupled to the two walls by film coefficients h. We then have

$$\frac{d\ T_R(t)}{dt} + \Lambda_R T_R(t) = \frac{1}{2} \Lambda_R \left[T_1(\xi_1 = 1,\ t) + T_2(\xi_2 = 0,\ t) \right] , \tag{2.10}$$

where $\Lambda_R = 2h/C_r$.

This description of a room is, of course, oversimplified and is presented here as a pedagogical aid in our description of the method. Nevertheless, one can interpret the outer "wall" as the average of the true outer wall plus roof and the inner "wall" as the average of the true 3 inner walls plus floor. These elements could all be treated separately without an undue increase in complexity if greater accuracy and flexibility are desired.

Equations (2.4 - 2.10) plus the condition of periodicity completely determine the temperatures of the model in terms of T_S. We first consider the time independent D.C. response. In this case, the temperatures are given by

$$T_1(\xi_1) = \eta_1\ T_{So}\ \xi_1 = \frac{S_o}{U_1} \xi_1 , \tag{2.11}$$

$$T_2(\xi_2) = (2 + \eta_1)\ T_{So} = \left(\frac{2}{h} + \frac{1}{U_1} \right) S_o, \tag{2.12}$$

$$T_{Ro} = (1 + \eta_1)\ T_{So} = \left(\frac{1}{h} + \frac{1}{U_1} \right) S_o, \tag{2.13}$$

where S_o is the $n = 0$ Fourier coefficient of the solar flux S(t).

From (2.13), we have

$$\chi_o = 1 + \eta_1. \tag{2.14}$$

We next consider the dynamic response of frequency $n\omega$. In this case, the equations yield, apart from a factor $e^{in\omega t}$,

$$T_1 = A \sinh k_1 \xi_1, \tag{2.15}$$

$$T_2 = B \cosh k_2 (1 - \xi_2), \tag{2.16}$$

with

$$k_j^2 = in\omega/\Lambda_j \quad , \quad j = 1,2, \tag{2.17}$$

and

$$A = \eta_1 T_R \Big/ [k_1 \cosh k_1 + \eta_1 \sinh k_1] , \tag{2.18}$$

$$B = \eta_2 (T_R + T_S) \Big/ [k_2 \sinh k_2 + \eta_2 \cosh k_2] , \tag{2.19}$$

with $T_R = \chi_n T_S$ and

$$\chi_n^{-1} = \left(1 + \frac{k_2}{\eta_2} \tanh k_2\right)\left(1 + \frac{2in\omega}{\Lambda_R} + \frac{1}{1 + \frac{\eta_1}{k_1} \tanh k_1}\right) - 1 \tag{2.20}$$

This completes the solution of the continuum model. Equations (2.14) and (2.20) are explicit examples of the general result (2.2).

Returning to the general development, we construct a simple lumped parameter model of the room temperature. We choose a model that consists of a heat capacity C coupled to the outside air through a conductance U and which is stimulated by a modified solar flux. The solar flux is modified by having a renormalized D.C. component. This modification decouples the static and dynamic aspects of the model and C and U affect only the dynamic aspects. The temperature of the heat capacity C, T, which is meant to model the room temperature T_R satisfies the equation

$$C \frac{dT}{dt} + UT = \alpha_o' S_o + (S - S_o) \tag{2.21}$$

where $\alpha_o' S_o$ is the modified D.C. component of the solar flux. We rewrite this equation as

$$\frac{dT}{dt} + \Lambda T = \Lambda\left[\alpha_o T_{So} + \alpha(T_S - T_{So})\right] , \tag{2.22}$$

where the new parameters are

$$\Lambda = \frac{U}{C} , \quad \alpha_o = \frac{h}{U}\alpha_o' , \quad \alpha = \frac{h}{U} . \tag{2.23}$$

The form of the model as described by equations (2.21) and (2.22) has been dictated by considerations of accuracy and efficiency. We have chosen a model with one relaxation time Λ^{-1} so that the resulting expressions for the temperature, as a function of time, will be simple and easy to use. This determines the form of the left-hand-side of the equation. The right-hand-side is the result of a compromise between taking the unmodified source S and the completely modified one

$$\sum_n \alpha_n' S_n e^{in\omega t} , \quad \text{with} \quad \alpha_n' = (in\omega C + U)\chi_n ,$$

which would yield the exact temperature. The compromise recognizes that there is a lot of heat capacity in passive solar structures, this heat capacity affects the dynamic but not the static response with the result that $\chi_0 >> |\chi_1| \cong |\chi_2|$, etc. Thus, it makes sense to treat the static response separately from the dynamic response. The separation also allows a more symmetrical determination of the parameters $-\alpha_0$ from the static response and Λ and α from the dynamic response.

These remarks can be amplified by considering a specific example. We consider case 2, see Table 2.1, which is discussed in more detail later on in this section. With α_0, α, and Λ chosen to minimize the root-mean square error of the model, see below, the model is in (RMS) error by 5.1% and the parameters are $\Lambda P = 3.27$, $C = 5.85$ BTU/ft^2 ^{o}F, and $U = 0.798$ BTU/ft^2 ^{o}F. However, if we do not modify S and require $\alpha_0 = 1$, then the model is in (RMS) error by 28% and the parameters are $\Lambda P = 0.63$, $C = 6.9$ BTU/ft^2 ^{o}F, and $U = 0.18$ BTU/ft^2 hr ^{o}F. This error is unacceptably large. The parameters are close to the continuum parameters $C_1 + C_2 + C_R = 12$ BTU/ft^2 ^{o}F and $U_1h/(U_1+h) =$ 0.091 BTU/ft^2 hr ^{o}F. This shows the dominant role played by the static response in determining these parameters which is evident from the magnitudes of χ_n, $|\chi_0| = 11$, $|\chi_1| = 0.565$, $|\chi_2| = 0.360$. Thus, the introduction of α_0 leads to a significant improvement of the model without any increase in complexity. We now turn to the determination of the parameters.

The accurate simulation of the average temperature is an important part of any model. We therefore choose α_0 so as to reproduce the average temperature exactly. From (2.2), we have $T_{Ro} = \chi_0 T_{So}$ and, from (2.2), we have $T_o = \alpha_0 T_{So}$. We therefore choose

$$\alpha_o = \chi_o. \tag{2.24}$$

In the model just discussed we would have from (2.14) $\alpha_o = 1 + \eta_1$. With this choice of α_o, the average temperature falls out of the problem and Λ and α can be chosen to model the dynamic part of the temperature. We choose them so as to minimize the mean square error defined by

$$e^2 = \frac{1}{T_o^2 P} \int_0^P dt \left[T(t) - T_R(t)\right]^2 \tag{2.25}$$

which is expressed as a fraction of the average temperature T_o. The minimization is most easily carried out in frequency space. We first solve (2.22) for the nonzero frequency components of T

$$\begin{aligned} T_n &= \frac{\alpha\Lambda}{\Lambda + in\omega} T_{Sn}, \qquad n \neq 0 \\ &= \frac{y}{x + in} T_{Sn} \ , \end{aligned} \tag{2.26}$$

where $x = \Lambda/\omega$ and $y = \alpha\Lambda/\omega$. We then use this result and (2.2) to write (2.25) as

$$e^2 = \frac{2}{T_o^2} \sum_{n=1}^{\infty} |T_{Sn}|^2 \left| \frac{y}{x + in} - \chi_n \right|^2 \tag{2.27}$$

which is to be minimized with respect to x and y.

Setting the derivative of (2.27) with respect to y equal to zero yields the equation

$$E_1(x)y = F_1(x) \tag{2.28}$$

and from $\partial e^2/\partial x = 0$, we get

$$E_2(x)xy = F_2(x), \tag{2.29}$$

where

$$E_\ell(x) = \sum_{n=1}^{\infty} \frac{s_n}{(x^2 + n^2)^\ell} , \quad \ell = 1,2, \tag{2.30}$$

and

$$F_\ell(x) = \mathrm{Re} \sum_{n=1}^{\infty} \frac{s_n \chi_n}{(x - in)^\ell} , \quad \ell = 1,2, \tag{2.31}$$

with

$$s_n = |T_{Sn} / T_o|^2 . \tag{2.32}$$

We get a single equation for x by dividing (2.29) by (2.28)

$$x = \frac{E_1(x)\ F_2(x)}{E_2(x)\ F_1(x)} . \tag{2.33}$$

This equation is discussed in more detail in the Appendix. Solving (2.33) for x, we then obtain y from

$$y = \frac{F_1(x)}{E_1(x)} . \tag{2.34}$$

The mean equare error at the minimum point is then given by

$$e^2 = 2\left[\sum_{n=1}^{\infty} s_n|\chi_n|^2 - \frac{F_1^2}{E_1}\right]. \tag{2.35}$$

The parameters x and y depend upon the shape of the time dependence of the heat source T_S through the presence of the magnitudes of the

Fourier coefficients in s_n in the sums E_ℓ and F_ℓ. For our example we chose T_S to be half of a sine wave which is 8 hours long, i.e.,

$$\begin{aligned} T_S(t) &= \sin \frac{3w}{2} t \quad , \quad 0 < t < \frac{P}{3} \quad , \\ &= 0 \quad , \quad \frac{P}{3} < t < P \quad , \end{aligned} \tag{2.36}$$

plus periodic extension. Note that the overall amplitude of T_S does not enter into our equations so we have set it equal to one. With this choice of T_S, we have

$$s_n = \frac{81}{32} \frac{\left(1 + \cos \frac{2\pi n}{3}\right)}{(n^2 - 9/4)^2} \tag{2.37}$$

Since s_n is proportional to n^{-4} for large n, the sums in (2.30) and (2.31) converge very fast. With this choice of s_n, we can proceed to solve (2.33) and 2.34) for x and y and calculate the root-mean-square error e from (2.35).

Our example is defined by X_n (2.20) and s_n (2.37). In Table 2.1, we list the values of the continuum parameters that were chosen for study and the resulting values of x, y, and e. The average RMS error of 7.8% for the four cases indicates that this method is sufficiently accurate for qualitative predictions. The most notable features of these results are the strong dependence of x and y on C_R and their weak dependence on C_2. In Table 2.2, we present the same results in the form of the lumped parameters U and C obtained from (2.23). Note that the values of U are very large compared to that of the outer wall plus film. This emphasizes the importance of separating static and dynamic responses. In Table 2.3, we compare the various decay constants of the continuum system with that of the lumped system. Here, λ is the decay constant of the slowest normal mode of continuum system. There are several important points to be noted from these numbers. First, since for all cases $\Lambda \gg \lambda$, we are not exciting just one normal mode which would make the good agreement indicated in Table 2.1 a rather weak test of the method. Second, we note that there is a very strong dependence of Λ on C_R but a very weak dependence on C_2.

The solution of Eq. (2.33) for x is straightforward but rather tedious unless it can be done on a computer. We therefore turn to a simple approximate solution which yields results that are not significantly worse than those obtained from (2.33). The approximation is based upon the observation that χ_n is a slowly varying function of n. We can therefore obtain approximate expressions for x and y by choosing them so that the n = 1 term in e^2, (2.27), is zero. This yields the simple results

$$x \cong \frac{\chi_1'}{\chi_1''} \quad , \qquad y \cong \frac{|\chi_1|^2}{\chi_1''} \tag{2.38}$$

which would also be obtained from (2.33) and (2.34) if only the first term in the sums (2.30) and (2.31) are kept. Values of x and y calculated from (2.38) and the associated root-mean-square errors are presented in Table 2.4. Comparing the values of e in this table with those in Table 2.1, we see that this approximation does not incur a serious penalty since it increases the error by an average of 0.7%.

For the sake of completeness, we conclude this section with expressions for T as a function of time. We take T_S as (2.36) so that T is given up to an everall scale factor by

$$T = \frac{2}{3\pi}(\alpha_o - \alpha) + \frac{iy}{x+\frac{3}{2}i}\left[\frac{i+e^{-2\Lambda P/3}}{1 - e^{-\Lambda P}} e^{-\Lambda t} - e^{3i\omega t/2}\right] \quad , 0 < t < \frac{P}{3}$$

$$= \frac{2}{3\pi}(\alpha_o - \alpha) + \frac{3}{2}\frac{y}{x^2+\frac{9}{4}}\ \frac{1+e^{+\Lambda P/3}}{1 - e^{-\Lambda P}} e^{-\Lambda t} \quad , \frac{P}{3} < t < P, \qquad (2.39)$$

plus periodic extension. This expression is the solution of (2.22) that is continuous and periodic with T_S given by (2.36). The real part of all complex expressions is implied. The parameter α_o equals 11 for all the cases we have treated and α = 0.93, 1.25, 0.72, 0.97 for cases 1 through 4 respectively. The other parameters can be read from the tables.

III. RESPONSE TO A HEATING PULSE

We now turn to the response of the room described in Sec. II to a heating pulse such as would be experienced at the beginning of a day during the heating season. Since the room temperature is a sum of terms with each term representing the response to a separate heat input, we can consider this problem separately from the one treated in the previous section. As a result, one may get very different lumped parameters for the response to each of the sources. Since these parameters are obtained by minimizing the RMS error in the modeled response to each of the sources separately and not the total RMS error in the presence of several sources, we are making the approximation that we can neglect cross-terms in the RMS error. Since this approximation decouples the determinations of the separate lumped parameters and renders them independent of the relative amplitudes of the various sources, it is crucial to the practical application of our method. This approximation will be accurate if we can model the response to each separate source to within our 10% criterion of accuracy.

The equations describing the room with a heater are only a slight modification of those given in Sec. II. Equations (2.4) - (2.7) and (2.9) are unchanged while (2.8) has $T_S = 0$ and there is an additional term $2T_H(t)$ inside the square brackets on the right-hand-side of (2.10) which represents the heater input. Here T_H is given by

$$T_H(t) = \frac{\dot{Q}(t)}{C_R \Lambda_R} = \frac{\dot{Q}(t)}{2h} \quad , \tag{3.1}$$

where $\dot{Q}$ is the rate of heat input per unit area from the heater. We will take $\dot{Q}$ to be a square pulse of height H and lasting from time t_0 to t_1. Recall that the day starts when the sunshine comes through the window, see (2.36). The Fourier coefficients of T_H are given by

$$T_{Hn} = \frac{e^{-in\omega t_0}}{2\pi in} \left[1-e^{-in\omega(t_1-t_0)}\right] \frac{H}{2h} \quad . \tag{3.2}$$

We might now proceed along the lines developed in Sec. II. That is, we might write the Fourier coefficients of the room temperature as $T_{Rn} = \chi_n T_{Hn}$ (this is Eq. (2.2) with a different χ_n) and solve for χ_n. We would then determine the optimum lumped parameters from equations similar to (2.33) and (2.34). This procedure yields results with unacceptably high errors--50% or more. The reason for this failure can be seen in Eq. (2.10) with a square-pulse source term on the right-hand-side. Depending upon the magnitude of Λ_R, T_R will try to follow this pulse with a quick rise and fast relaxation in times of the order of $1/\Lambda_R$. At the same time T_R is driven by the terms T_1 and T_2 on the right-hand-side of (2.10) which typically change over periods characteristic of the walls which are much longer than $1/\Lambda_R$. Thus, the reason for the breakdown of the method in this case is that we are trying to model a system that has two drastically different time scales with one time constant. We therefore have to modify our method so as to eliminate one of the time scales before proceeding as in Sec. II.

In order to eliminate rapidly changing part of T_R, we split it into two parts, a direct part T_R^d and an indirect part T_R^i, as

$$T_R(t) = T_R^d(t) + T_R^i(t) \quad . \tag{3.3}$$

The direct part is defined to be the periodic solution of the equation

$$\frac{dT_R^d}{dt} + \Lambda_R T_R^d = \Lambda_R T_H \quad , \tag{3.4}$$

and the indirect part is the solution of Eq. (2.10). The direct term now plays the role of a source for the indirect term since it appears in (2.6) and (2.8) when (3.3) is used for T_R. We can then write the relation between the Fourier coefficients of T_R^i and T_R^d as $T_{Rn}^i = \chi_n T_{Rn}^d$ and proceed as in Sec. II. This means that we must also split the lumped-parameter-model temperature into direct and indirect parts as in (3.3), i.e.,

$$T(t) = T^d(t) + T^i(t) \tag{3.5}$$

with

$$T^d(t) = T_R^d(t) \tag{3.6}$$

and T^i determined by Eq. (2.22) with T_S replaced by T_R^d. Since the RMS error (2.25) depends upon the difference between T and T_R the direct parts cancel due to (3.6) and we are left with the problem of determining the optimum lumped parameters for the indirect part which can be well simulated with one time constant. We first determine T_R^d from (3.4) and then χ_n from the modified Eqs. (2.4) - (2.10). These results can then be used in (2.33) and (2.34) to determine the values of the optimum lumped parameters.

We solve Eq. (3.4) using (3.1) for T_H and requiring continuity and periodicity. We then get

$$T_R^d(t) = \frac{H}{2h}\left[\frac{1-e^{-\Lambda_R(t_1-t_0)}}{1-e^{-\Lambda_R P}}\right] e^{-\Lambda_R(P-t_1+t)}, \quad 0 < t < t_0,$$

$$= \frac{H}{2h}\left\{1-\left[\frac{1-e^{-\Lambda_R(P+t_0-t_1)}}{1-e^{-\Lambda_R P}}\right] e^{-\Lambda_R(t-t_0)}\right\}, \quad t_0 < t < t_1,$$

$$= \frac{H}{2H}\left[\frac{1-e^{-\Lambda_R(t_1-t_0)}}{1-e^{-\Lambda_R P}}\right] e^{-\Lambda_R(t-t_1)}, \quad t_1 < t < P. \tag{3.7}$$

The Fourier coefficients of T_R^d can be read directly from (3.4) and (3.2) or calculated from (3.7) with the result

$$T_{Rn}^d = \frac{\Lambda_R e^{-in\omega t_0}}{2\pi in(\Lambda_R+in\omega)}\left[1-e^{-in\omega(t_1-t_0)}\right]\frac{H}{2h} \quad . \tag{3.8}$$

This is to be used as the source for T_R^i.

The solutions for T_1 and T_2 given in (2.15) and (2.16) are still valid and the constants A and B are given by (2.18) and (2.19) with $T_S = 0$ and T_R given by (3.3) and (3.8). These results are then substituted into (2.10), with T_R replaced by T_R^i, which is then solved for $T_{Rn}^i = X_n T_{Rn}^d$ with the result,

$$X_n^{-1} = 2\left(1+\frac{in\omega}{\Lambda_R}\right)\left(\frac{1}{1+\frac{k_1}{\eta_1}\coth k_1} + \frac{1}{1+\frac{k_2}{\eta_2}\tanh k_2}\right)^{-1} -1 \quad . \tag{3.9}$$

As a check on this expression, we may verify that they give the correct zero-frequency results. From (3.8) we have $T_{R0}^d = (t_1-t_0)H/2Ph$ and from (3.9) we have $X_0 = 1+2\eta_1$. We then have

$$T_{R0} = (1+X_0)T_{R0}^d = \frac{H(t_1-t_0)}{P}\left(\frac{1}{h}+\frac{1}{U_1}\right)$$

which is the expected result.

The lumped parameters U and C can now be obtained from x and y given by (2.33) and (2.34) with χ_n given by (3.8) and s_n given by

$$s_n = \left| T^d_{Rn}/T_0 \right|^2$$

$$= \frac{1}{4(1+\eta_1)^2 \left[1+\left(\frac{n\omega}{\Lambda_R}\right)^2\right]} \left[\frac{\sin \frac{n\omega}{2}(t_1-t_0)}{\frac{n\omega}{2}(t_1-t_0)}\right]^2 . \qquad (3.10)$$

The mean-square error is given by (2.35) and α_o is given by (2.24) plus the above zero frequency results, $\alpha_o = 1+2\eta_1$.

In Tables 3.1 - 3.3, we present some numerical examples of the above procedure. We have chosen the room parameters to be the same as the four cases treated in Sec. II so that the strong process dependence of the optimum lumped parameters is demonstrated. We have also chosen two pulse durations--a short pulse 1/4 hour long and a long pulse 1 hour long--in order to illustrate the dependence on this parameter.

In Table 3.1, we present the calculated values of x, y, and the RMS error for the eight cases that we have treated. These numbers show a very strong dependence on C_R as one would expect. Furthermore, there is a strong dependence on the pulse duration when $C_R = 0$ but a very weak dependence when $C_R = 1$ BTU/^{o}F ft^2. The RMS errors are all in or near our acceptable range. It should be pointed out that if we do not separate the room temperature into a direct and indirect part, (3.3), but try to simulate the room temperature with a single time constant such as was used in Sec. II, then these errors are increased by roughly a factor of 10. This would place us well outside the acceptable range. Thus, the utility of the separation (3.3) has been demonstrated.

In Table 3.2, we present the dimensional lumped parameters U and C and the decay constant Λ. Here one sees striking differences between these values and those given in Tables 2.2 and 2.3 for the passive solar room. One also sees that the heat capacity C_R has a very strong effect on the value Λ.

In Table 3.3, we present results obtained using the approximation (2.38) for x and y. Here, we see that the resultant values of x and y can be very different from those given in Table 3.1. This is a reflection of the importance of higher harmonics of the fundamental frequency in this modeling. The errors given in this table are satisfactory in many cases. Thus, this approximation can be used to obtain a rough idea of the temporal development of the temperature.

IV. CONCLUSION

We have presented a method for constructing simple lumped parameter models of thermal structures that are subjected to periodic sources of heat. The method was applied to two examples to explore its domain of applicability. The first example was intended to simulate a room with passive solar heating and the second was a room subjected to a square wave pulse of heat. The method is quite general and can be used to model any thermal system that is subjected to a periodic stimulus. One must first calculate the relative spectral weights s_n of the stimulus and the temperature susceptibility χ_n of the system. The lumped parameters then follow from Eqs. (2.33) and (2.34). The resulting temperature is the "best" in the least squares sense. We present below some comments on the dependence of the parameters on the shape of the stimulus, parameter dependence of the accuracy of the method, the utility of introducing more complicated lumped parameter models with more than one decay constant, and the possibility of modeling systems whose parameters change discontinuously.

The approximation (2.38) for x and y is a shape independent approximation since it yields results that are independent of the shape of T_S as reflected in the values of s_n. This approximation gave accurate results for the example treated in Sec. II and one would therefore expect that x and y are insensitivie to changes in the shape of T_S within the domain of "reasonable" shapes. This conjecture was tested by considering a source whose shape was an 8 hour square wave,

$$T_S(t) = 1 \ , \ 0 < t < \frac{P}{3} \ ,$$

$$= 0 \ , \ \frac{P}{3} < t < P \ , \tag{4.1}$$

rather than the 8 hour semisine wave given by (2.36). This stimulus has relatively stronger high frequency components (s_n is proportional to n^{-2} rather than n^{-4} for large n). Numerical studies show that the lumped parameters are insensitive to this change in stimulus. However, the RMS error is somewhat less for the square wave than it is for the semisine wave. This reflects a corresponding reduction in the variation of the temperature about its mean value.

The situation is somewhat different for the heater pulse modeled in Sec III. There we see that the validity of the shape-independent approximation depends upon the presence of a room heat capacity. The values of x and y as well as the error e are substantially different for cases 1 and 3 under this approximation, Table 3.3, than the exact values given in Table 3.1. However, the approximation seems to work well for nonzero room heat capacity, cases 2 and 4.

We have chosen a value for U_2 of the inner wall that leads to a substantial variation in the room temperature. The RMS variation of the room temperature about its mean is typically 63-98% for the examples treated. Larger values of U_2 would lead to a smaller variation of the temperature and a less demanding test of the method.

It is possible to improve the accuracy of the lumped model by coupling additional heat capacities to the one whose temperature models that of the room. The new parameters characterizing these heat capacities could be determined by minimizing the RMS error in the model temperature. However, these new parameters are liable to be very inefficient since they introduce substantial complications into the calculations and cannot be expected to make dramatic improvements in the accuracy. The complications come about both in the determination of the parameters and in the representation of the temperature as a function of time. The improved accuracy cannot be more than one or two percent per additional heat capacity since a single heat capacity gives results that are within 10% of the exact results. Thus, the introduction of additional parameters would only be justified under special circumstances.

Systems whose parameters change discontinuously, e.g., the closing of shutters at night, cannot be easily treated by Fourier techniques. Therefore, our methods cannot be directly applied to them. However, our method can be used to determine optimum lumped parameters for each value of the system parameters and these could then be used to model the system temperature. The accuracy of this approach requires further investigation.

We conclude that the method we have presented for developing lumped parameter models of complex thermal structures is both practical and accurate.

References

1. For examples, see T. Kusuda, NBSLD, The Computer Program for Heating and Cooling Loads in Buildings, NBS Bldg. Sci. Series, 69 (1976); E. Shaviv and G. Shaviv, Modeling the Thermal Performance of Buildings, Buildings and Environment 13, 95 (1978); F. Arumi-Noe and D. O. Northrup, A Field Validation of the Thermal Performance of a Passive Heated Building as Simulated by the DEROB System, Energy and Buildings 2, 65 (1979).
2. F. Kreith, Principles of Heat Transfer, Intext Educational Publishers, New York, 1973; J. L. Threlkeld, Thermal Environmental Engineering, Prentice-Hall Publishing Co., Englewood Cliffs, New Jersey, 1970, Ch. 14.
3. R. Bruno, U. Brombach, and B. Steinmuller, On Calculating Heating and Cooling Requirements, Energy and Buildings 2, 197 (1979).

APPENDIX: ANALYSIS OF EQUATION (2.33)

Some insight into the structure of Eq. (2.33) can be obtained by generalizing x to a complex variable z and studying the analytic properties of the functions involved. However, as a practical matter, the equation is most easily solved by calculating the functions directly from their definitions (2.30) and (2.31).

In order to study the analytic structure of (2.33), we introduce two new functions

$$E(x) \equiv \frac{E_2(x)}{E_1(x)} = -\frac{1}{2x}\frac{d}{dx}\ln E_1(x)$$

$$F(x) \equiv \frac{F_2(x)}{F_1(x)} = -\frac{d}{dx}\ln F_1(x) \tag{A.1}$$

and generalize x to a complex variable z. Since $E_1(z)$ and $F_1(z)$, Eqs. (2.30) and (2.31), are meromorphic functions, E and F will also be meromorphic. Furthermore, the poles of E(F) will be located at the poles and zeros of $E_1(F_1)$ and the residues of the ploes of the logarithmic derivatives will be plus or minus one. With this information, we can write down alternate expressions for E and F

$$E(z) = \sum_{m=1}^{\infty} \frac{1}{z^2+m^2} - \sum_{\ell=1} \frac{1}{z^2+\xi_\ell^2}\ , \tag{A.2}$$

$$F(z) = 2z\sum_{m=1}^{\infty} \frac{1}{z^2+m^2} - \frac{1}{z-\zeta_0} - \sum_{\ell=1}^{\infty}\left(\frac{1}{z-\zeta_\ell} + \frac{1}{z-\zeta_\ell^*}\right) \tag{A.3}$$

where $\pm i\xi_\ell$ are roots of the equation

$$E_1(z) = \sum_{n=1}^{\infty} \frac{s_n}{z^2+n^2} = 0, \tag{A.4}$$

and ζ_0, ζ_ℓ, and ζ_ℓ^* are roots of the equation

$$F_1(z) = \frac{1}{2} \sum_{n\neq 0} \frac{s_n \chi_n}{z-in} = 0. \tag{A.5}$$

We can use the functions E and F to rewrite (2.33) as $xE(x) = F(x)$, or using (A.2) and (A.3) as

$$\frac{\pi}{2} \coth \pi x - \frac{1}{2x} + x\sum_{\ell=1}^{\infty} \frac{1}{x^2+\xi_\ell^2} - \frac{1}{x-\zeta_0} - \sum_{\ell=1} \left(\frac{1}{x-\zeta_\ell} + \frac{1}{x-\zeta_\ell^*} \right) = 0 . \tag{A.6}$$

where we have used

$$\sum_{m=1}^{\infty} \frac{1}{z^2+m^2} = \frac{\pi}{2z} \coth\pi z - \frac{1}{2z^2} \tag{A.7}$$

Thus, all the effects of the stimulus s_n and the system χ_n are contained in the roots of Eqs. (A.4) and (A.5).

It is easy to show that the roots of (A.4) are real and lie in the intervals $\ell < \xi_\ell < \ell-1$. Furthermore, we can write an explicit expression for $E_1(z)$ in terms of the stimulus as follows: we write

$$E_1(z) = \frac{1}{P} \int_0^P dt\; G^2(t, z), \tag{A.8}$$

where G is the continuous and periodic solution of the equation

$$\frac{dG}{dt} + \omega zG = \frac{\omega}{T_{SO}} \left[T_S(t) - T_{SO} \right] . \tag{A.9}$$

This equation can be solved an an expression for E_1 obtained for any specific $T_S(t)$. The roots of this expression can then be easily calculated. It is difficult to say anything generally true about the roots of (A.5) since they are complex roots of a complex equation.

TABLE 2.1. Continuum parameters and resultant solutions of Eqs. (2.33) and (2.34) for passive solar room. The U's and h are given in Btu/^{o}F-hr-ft^{2} and the C's in Btu/^{o}F-ft^{2}. The RMS error e is given in percent of the mean.

case	h	U_1	C_1	U_2	C_2	C_R	x	y	e
1	1	0.1	1	0.5	10	0	1.085	1.006	14.2
2	1	0.1	1	0.5	10	1	0.521	0.653	5.1
3	1	0.1	1	0.5	20	0	1.066	0.766	9.2
4	1	0.1	1	0.5	20	1	0.537	0.521	2.7

TABLE 2.2. The lumped parameters U and C for passive solar room. See Table 2.1 for cases and units.

Case	U	C
1	1.079	3.797
2	0.798	5.849
3	1.392	4.987
4	1.031	7.332

TABLE 2.3. Decay constants for passive solar room. See Table 2.1 for cases.

Case	$\Lambda_1 P$	$\Lambda_2 P$	λP	ΛP
1	2.4	1.2	0.186	6.817
2	2.4	1.2	0.173	3.274
3	2.4	0.6	0.094	6.698
4	2.4	0.6	0.090	3.374

TABLE 2.4. Approximate values of x and y calculated from Eq. (2.38) and associated root-mean-square errors e expressed as a percentage of the mean for passive solar room. See Table 2.1 for cases.

Case	x	y	e
1	0.943	0.919	15.7
2	0.505	0.633	5.5
3	0.956	0.719	10.0
4	0.528	0.511	2.9

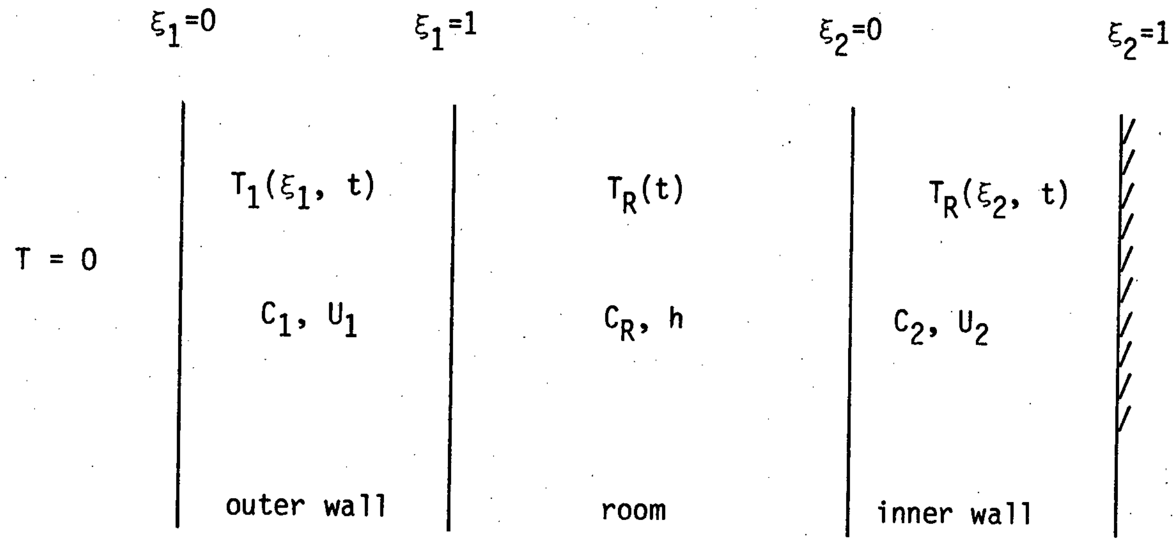

Fig. 2.1. Configuration of simplified room with passive solar heating.

TABLE 3.1. Solutions to Eqs. (2.33) and (2.34) and RMS errors for a heat pulse of duration τ (hours). See Table 2.1 for cases.

τ	1/4			1		
Case	x	y	e	x	y	e
1	15.82	16.53	12.6	5.626	8.440	7.8
2	1.017	2.426	1.7	1.001	2.403	1.6
3	20.15	17.52	10.7	7.082	8.689	6.7
4	1.172	2.299	1.5	1.158	2.275	1.4

TABLE 3.2. The lumped parameters U and C and the decay constants for a heat pulse of duration τ (hours). See Table 2.1 for cases and units.

τ	1/4			1		
Case	U	C	ΛP	U	C	ΛP
1	0.957	0.231	99.4	0.667	0.453	35.3
2	0.419	1.574	6.39	0.417	1.590	6.29
3	1.150	0.218	126.6	0.815	0.440	44.5
4	0.510	1.661	7.36	0.509	1.679	7.28

TABLE 3.3. Approximate values of x and y calculated from Eq. (2.38) and associated root-mean-square errors e expressed as a percentage of the mean for a heat pulse of duration τ (hours). See Table 2.1 for the cases.

			e	
Case	x	y	$\tau=1/4$	$\tau=1$
1	1.519	3.422	20.6	12.0
2	0.843	2.078	2.5	2.3
3	1.704	3.218	18.9	10.7
4	0.957	1.957	2.2	2.0

TECHNICAL INFORMATION DEPARTMENT
LAWRENCE BERKELEY LABORATORY
UNIVERSITY OF CALIFORNIA
BERKELEY, CALIFORNIA 94720